MECHANISMS OF CRACK PROPAGATION DUE TO CORROSION IN CONCRETE

Farid UDDIN A.K.M.*[1] Kazuhito ISHIHARAGUCHI*[1] and Masayasu OHTSU*[2]

ABSTRACT: Due to expansion of corrosive products, cracks are nucleated around reinforcement in concrete. Initiation and propagation of these cracks are studied by experimentally and analytically. Crack kinematics in fracture process zone are determined by AE-SiGMA (**Si**mplified **G**reen's function for **M**oment tensor **A**nalysis) code. Simulation of crack propagation due to corrosion is carried out by the two-domain boundary element method (BEM). In the analysis, the ratios of stress intensity factors of mode I to mode II (K_I/K_{II}) are determined for the different types of crack patterns. These analytical results are compared with the results of the SiGMA analysis.

KEYWORDS: crack propagation, boundary element method (BEM), acoustic emission (AE), stress intensity factors, SiGMA code

1. INTRODUCTION

Corrosion cracking in concrete is generated due to expansion of corrosive products. Crack propagation in cementitious materials has been intensively studied on the basis of fracture mechanics. Acoustic emission (AE) techniques have been extensively studied in concrete engineering, where it is known that one promising approach is the application of AE to fracture mechanics. Based on fundamental research, to classify crack types and to determine crack orientations, the moment tensor analysis is implemented as the SiGMA (Simplified Green's function for Moment tensor Analysis) code[1,2].

In the present paper, crack propagation due to corrosion of reinforcement is studied. The two-domain boundary element method (BEM) is applied to trace crack extension based on the linear elastic fracture mechanics (LEFM)[3]. Crack kinematics is clarified by applying the SiGMA analysis and compared with results of the BEM analysis.

2. CRACK KINEMATICS BY AE

A crack can be modeled by crack-motion vector **b** and unit normal vector **n** to crack surface F. Crack motion is set to be $b(\mathbf{y})\boldsymbol{l}S(t)$, where $b(\mathbf{y})$ represents the magnitude of crack displacement, $\boldsymbol{l}$ is the direction vector of crack motion, and S(t) is the source-time function of crack motion. From a generalized theory[1], AE wave motion $\mathbf{u}(\mathbf{x},t)$ can be represented,

$$\mathbf{u}_i(\mathbf{x},t)=\int_F C_{pqkl}G_{ip,q}(\mathbf{x},\mathbf{y},t)*[b(\mathbf{y})\mathbf{l}_k S(t)n_l]dS=G_{ip,q}(\mathbf{x},\mathbf{y},t)m_{pq}*S(t), \quad (1)$$

where $G_{ip,q}$ is the spatial derivative of Green's function and the following integration over crack surface F leads to the moment tensor m_{pq},

$$\int_F C_{pqkl}[b(\mathbf{y})l_k n_l]dS=[C_{pqkl}\, l_k\, n_l][\int_F b(\mathbf{y})dS]=[C_{pqkl}\ \ l_k\, n_l]\Delta V=m_{pq} \quad (2)$$

In the case of an isotropic elasticity,

$$m_{pq} = (\lambda\ l_k n_l \delta_{pq} + \mu l_p n_q + \mu l_q n_p)\Delta V \quad (3)$$

---

*1Graduate Student, Graduate School of Science and Technology, Kumamoto University, Member of JCI
*2 Professor, Graduate School of Science and Technology, Kumamoto University, Dr. E., Member of JCI

Here λ and μ are Lame constants, and the summation convention is employed. In the SiGMA code[2)], **Eq.1** is simplified, taking into account only the first motion A(x) of AE waveform,

$$A(x)=Cs/R \; Ref \; (t,r) \; r_p \; m_{pq} \; r_q, \tag{4}$$

where Cs is the calibration coefficient, R is the distance, and it direction vector is **r**. Ref is the reflection coefficient. Since the moment tensor is symmetric and of the 2nd order, the number of independent unknown components m_{pq} is six. To solve **Eq.4**, two parameters of the arrival time and the amplitude of the first motion are read visually from recorded AE waveforms, by displaying them on the CRT. The location of the source is determined from the arrival time differences. Then, **Eq.4** is solved to determine moment tensor components m_{pq}. It is noted that, prior to the solutions, calibration coefficient Cs in **Eq.4** should be relatively determined to compensate the sensitivity of AE sensors.

The eigenvalue analysis of the moment tensor is performed. Setting shear contribution of the moment tensor as X, three eigenvalues e_1, e_2, and e_3 of the pure shear crack become (X, 0, -X) because $l_k n_k=0$. In the case of the pure tensile crack, three eigenvalues are decomposed into the deviatoric components (Y, -Y/2, -Y/2) and the isotropic components (Z, Z, Z), setting the maximum deviatoric tensile component as Y and the isotropic tensile component as Z. In the case of a general crack, it is assumed that the eigenvalues of the moment tensor are composed of the shear crack and the tensile crack. Thus, for the classification of crack, **Eq.5** is obtained as,

$$\begin{aligned} 0 &= X + Y + Z \\ e_2 / e_1 &= 0 - 0.5Y + Z \\ e_2 / e_1 &= -X - 0.5Y + Z \end{aligned} \tag{5}$$

AE sources for which the shear ratios X are smaller than 40% are classified as tensile cracks. AE sources of the shear ratio X greater than 60% are referred to as shear cracks.

3. EXPERIMENTS

Mixture proportion of concrete was made up as water (W): cement (C): sand (S) : gravel (G) = 0.5: 1.0:2.41:2.95 by weight. The maximum size of aggregate was 20mm. Slump value and air content were 8.0 cm and 5.0%, respectively. By making a slab specimen (dimension: 25cmX25cmX10cm), an experiment was carried out to simulate corrosion cracking. The compressive strength at 28days was 37.9MPa.

To simulate corrosion cracking of mixed mode in concrete, an expansion experiment was conducted. Cracks due to corrosion of reinforcements are generated in the long process and very difficult to examine in the short time. Thus, hydrostatic radial pressure was introduced by employing expansive agent. Crack patterns observed in the experiment are shown in **Fig.1**. The crack traces are denoted by mark A, B, and C. These crack traces are analyzed by BEM.

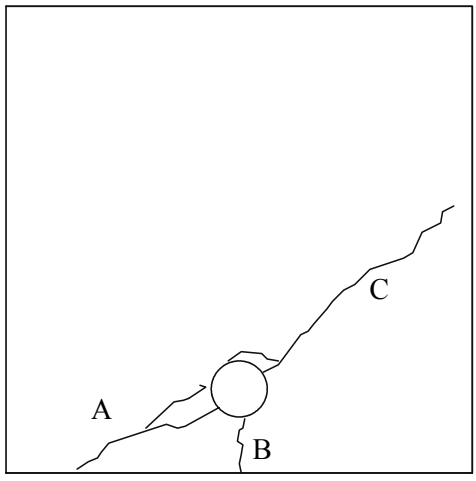

Fig.1 Observed crack patterns in the experiment

4. CRACK ANALYSIS BY BEM

In BEM, the governing equation is converted into the integral form on the boundary. After solving boundary integral equations in respect to tractions and displacements on boundary, stresses at arbitrary locations are determined for the stress analysis. A basic equation of BEM is represented as,

$$\tfrac{1}{2}u_i(x)=\int_S [U_{ij}(x,y)t_j(y)-T_{ij}(x,y)u_j(y)]dS \tag{6}$$

where $u_i(x)$ and $u_j(y)$ are the displacements and $t_j(y)$ is the traction. Point y is always located on the boundary S.

In this research, the domain is divided into two, which are stitched at the interface. **Eq.6** is applied to each domain and discretized. A typical two-domain model for the analysis of crack propagation is shown in **Fig.2**. At each step of the analysis, the stress intensity factor at the crack tip is computed from the displacements of the crack-tip elements. When a crack propagates, the node at the crack tip is separated into two nodes, creating new stress-free elements in the direction θ. The stitching interface is created, connecting the crack tip with the termination point **T** in **Fig.2**.The direction of the maximum tangential stress θ is determined by Erdogan-Sih criterion[4]:

$$K_I \sin\theta + K_{II}(3\cos\theta - 1) = 0 \tag{7}$$

$$\cos\frac{\theta}{2}\left[K_I \cos^2\left(\frac{\theta}{2}\right) - \frac{3}{2}K_{II}\sin\theta\right] = K_{IC}, \tag{8}$$

where K_I and K_{II} are the stress intensity factors of mode I and mode II, respectively. K_{IC} is the critical stress intensity factor previously determined[5] and is equal to 0.723MPa $m^{1/2}$. In **Fig.2**, a circle of 3.0cm diameter represents the location of the reinforcement, where the expansive pressure was applied by dolomite paste in the experiment. Crack trace A, B, and C in **Fig.1** are separately modeled as in **Fig.2**.

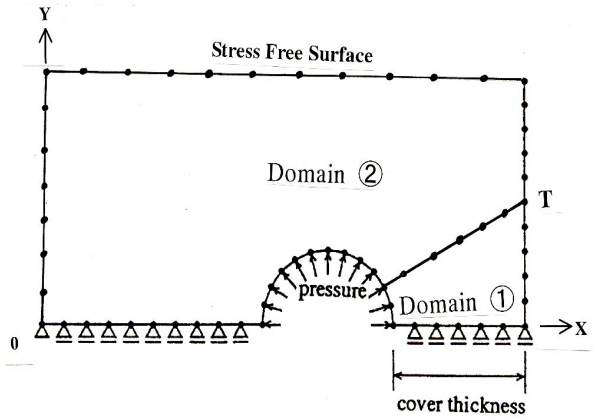

Fig. 2 Two-domain BEM model

5. RESULTS AND DISCUSSION

Crack traces A, B, and C in **Fig.1** are analyzed by BEM. All AE sources analyzed by the AE-SiGMA analysis are classified into three groups related with the three crack traces. The classification is conducted visually. Results are discussed, as follows:

5.1 CRACK TRACE A

Crack trace A is analyzed with the stress free boundary condition at the cover thickness, because crack trace A is observed after crack trace B. In BEM analysis, reasonable agreement is observed between

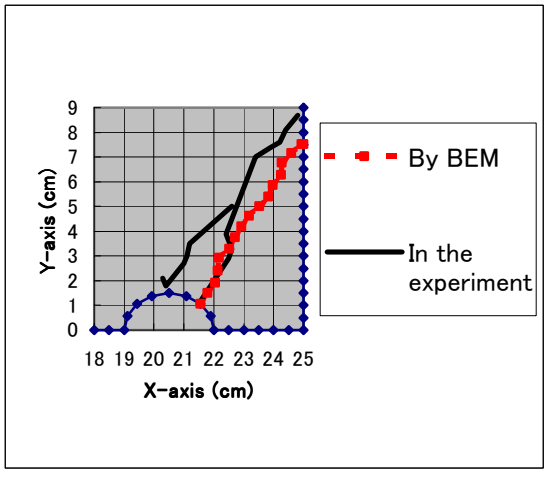

Fig.3 Crack traces A

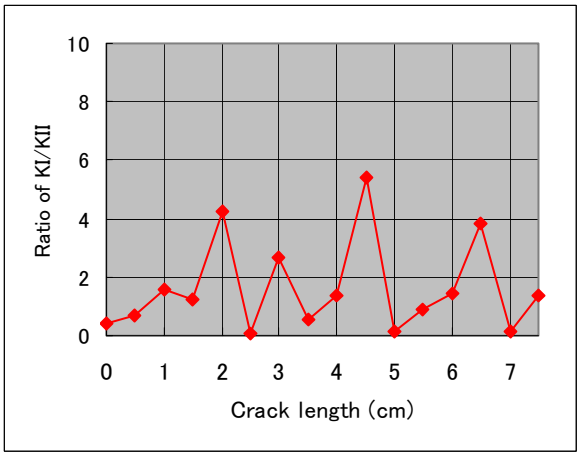

Fig.4 Ratios K_I/K_{II} during crack extension (trace A)

actual crack trace in the experiment and that of BEM crack trace as shown in **Fig.3**. Then, ratios of stress

intensity factors of mode I to mode II (K_I/K_{II}) determined from **Eq.7** are plotted with the increment of crack extension, as shown in **Fig.4**. The ratios start less than 1.0 and then higher ratios are mostly observed. This indicates that the crack extension is globally dominated by the mode-I fracture became the ratio is higher than 1.0, namely $K_I > K_{II}$.

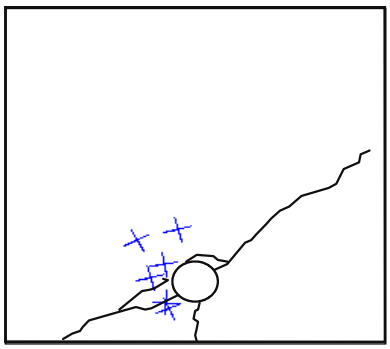

Fig.5 Locations of shear cracks during crack extension (trace A)

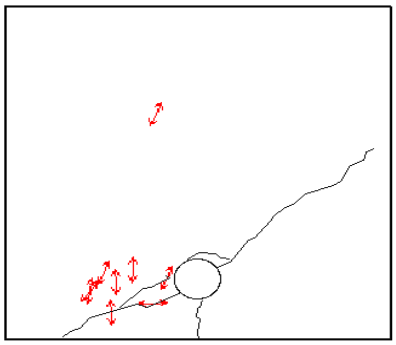

Fig.6 Locations of tensile cracks during crack extension (trace A)

From AE-SiGMA analysis, it is observed that both tensile and shear cracks occur as seen in **Figs.5** and **6**. Concerning shear cracks, directions of a crack vector and a crack normal are indicated by the cross (×) symbol. Tensile cracks are located at their location with the crack-opening direction by the arrow symbol (↔). Occurrence of these cracks is summarized in **Fig.7**. It is observed that in beginning of crack extension shear cracks are slightly dominant and finally tensile cracks dominate. From these two analyses, it can be concluded on crack trace A that tensile cracks mostly dominate shear cracks, although mixed-mode cracks are somehow observed.

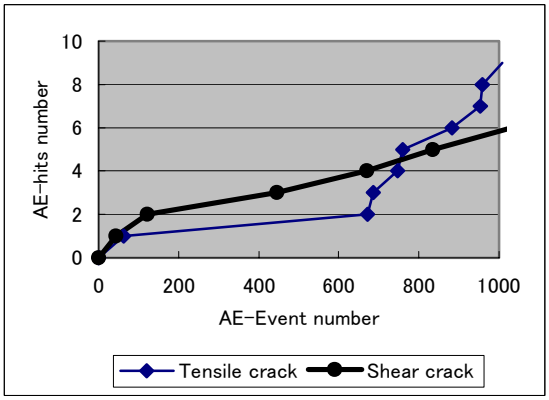

Fig.7 AE activities during crack extension (trace A)

5.2 CRACK TRACE B

There is a good agreement between actual crack in the experiment and BEM crack trace as shown in **Fig.8**. Ratios of stress intensity factors are plotted with the increment of crack extension as shown in **Fig.9**. The ratios start with almost equal to greater than 1.0 and then lower and higher ratios are observed.

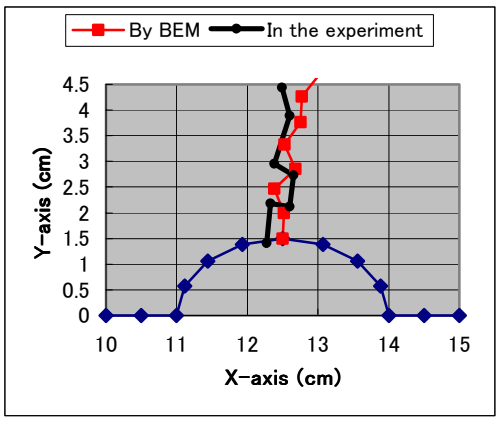

Fig.8 Crack traces B

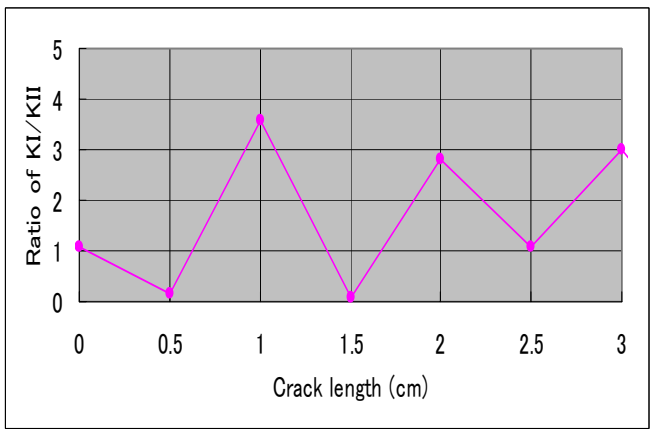

Fig.9 Ratios K_I/K_{II} during crack extension (trace B)

This indicates that the crack starts with the mode I. Crack extension is mostly of mode I as $K_I/K_{II}>1.0$

It is observed from **Figs.10** and **11** that tensile cracks are clearly generated close to crack trace B, while shear cracks are little far from the trace. According to **Fig.12**, it is observed that tensile cracks are always active. From these two analyses, it can be concluded that during extension of crack trace B tensile cracks mostly dominate shear cracks. Crack initiation results from the mode-I fracture, resulting in interaction with mode II.

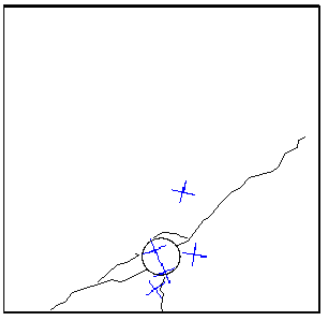

Fig.10 Locations of shear cracks during crack extension (trace B)

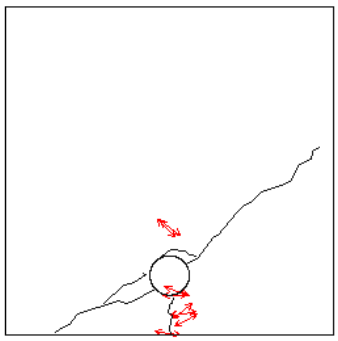

Fig.11 Locations of tensile cracks during crack extension (trace B)

5.3 CRACK TRACE C

Crack traces are compared in **Fig.13.** It is observed that the ratios of stress intensity factors (K_I/K_{II}) are mostly less than 1.0 as shown in **Fig.14**. This indicates that the crack propagates with almost mode-II fracture. Only in the beginning and the final stage, the larger ratios are observed. This result reveals that the mode-II fracture dominates during extension of crack trace C. It is observed from **Figs.15** and **16** that both tensile and shear cracks occurred along the trace.

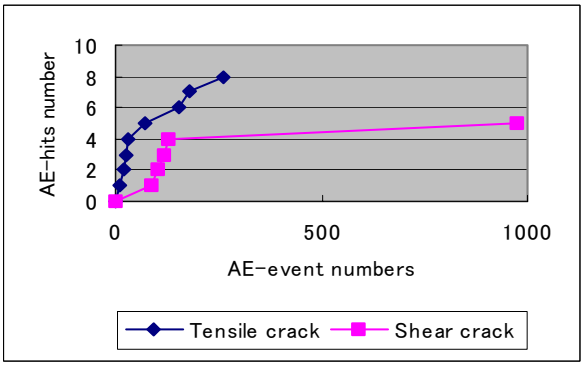

Fig.12 AE activities during crack extension (trace B)

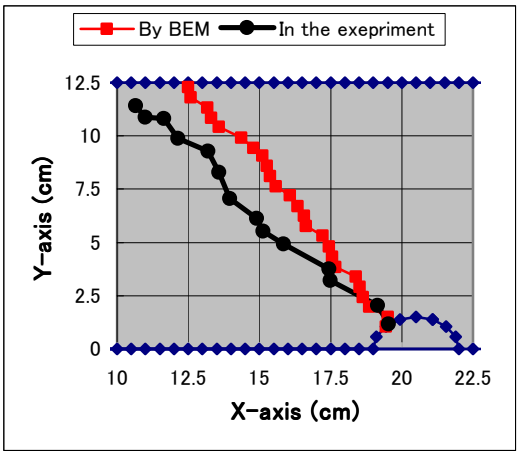

Fig.13 Crack traces C

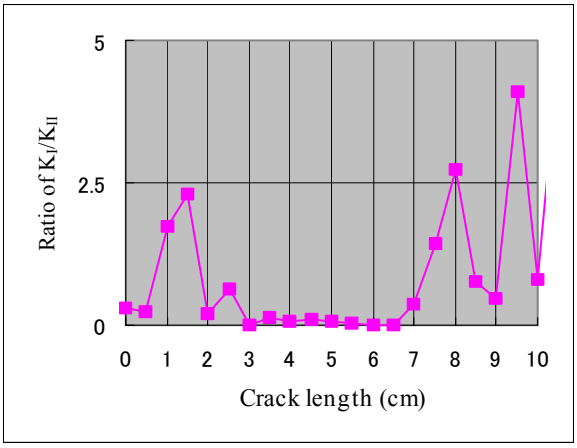

Fig.14 Ratios K_I/K_{II} during crack extension (trace C)

From **Fig.17**, it is clearly observed that in crack trace C, shear cracks are always dominant. These results clearly indicate that crack nucleation results from the mode-II fracture.

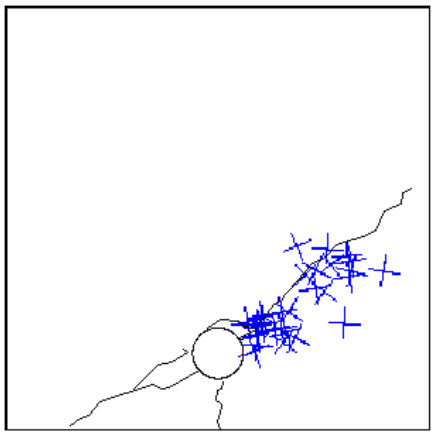

Fig.15 Locations of shear cracks during crack extension (trace C)

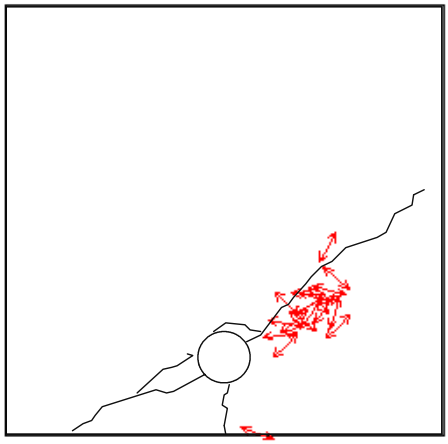

Fig.16 Locations of tensile cracks during crack extension (trace C)

6. CONCLUSION

Crack propagation due to corrosion of reinforcement in concrete is studied numerically and experimentally. Results are concluded, as follows:

(1) The analytical results by BEM are in reasonable agreement with experimental results. The ratios of stress intensity factors (K_I/K_{II}) are studied from the results of BEM analysis.

(2) Crack kinematics of the crack traces observed are investigated by AE-SiGMA analysis.

(3) It is found that cracking mechanisms due to corrosion of reinforcement: mode-I is dominant in the spalling crack (trace A) and the surface crack (trace B), while mode-II is dominant in the internal crack (trace C).

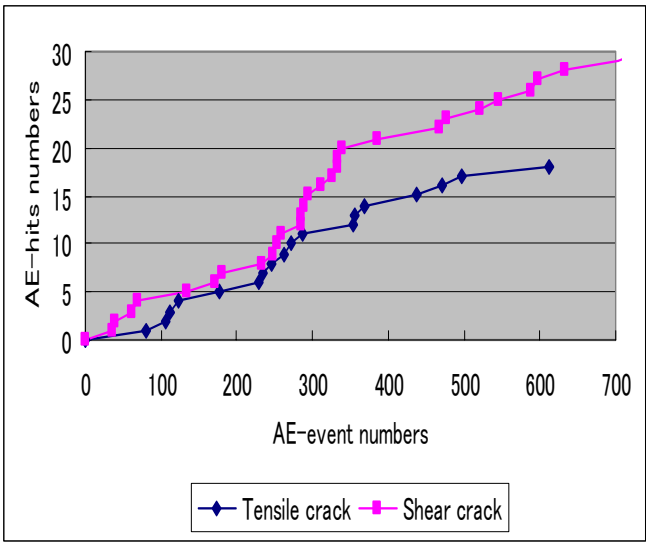

Fig.17 AE activities during crack extension (trace C)

REFERENCE

1. Ohtsu, M., "Source mechanism and Waveform Analysis of Acoustic Emission in Concrete," J. of AE, 2(1), 1982, pp.103-112
2. Ohtsu, M., "Simplified Moment Tensor Analysis and unified decomposition of AE source," J of Geophys. Res. 1991; 96:6211-6221
3. Chahrour, A.H., Fukuchi, S., Ohtsu, M. and Tomoda, Y., "BEM Analysis of Mixed-Mode Crack Propagation in Center-Notched Concrete Beams," Transactions of JCI, Vol.15, Dec. 1993, pp. 201-208
4. Erdogan, F. and Sih, G.C., "On the Crack Extension in Plates under Plane Loading and Transverse Shear," J. of Basic Eng., No.12, Dec. 1963, pp.519-527
5. Farid Uddin A.K.M., K. Ishiharaguchi and M. Ohtsu, "Stress Intensity Factors by Acoustic Emission and Analysis of Crack Propagation by Boundary Element Method," Proceeding of the 15th International AE Symposium, Progress in AE X, Sep. 2000, pp.11-16